EXTENDING OFDM SYMBOLS TO REDUCE POWER CONSUMPTION

André B. J. Kokkeler and Gerard J. M. Smit

Department of Computer Science, Electrical Engineering and Mathematics, University of Twente,
PO Box 217, 7500 AE Enschede, The Netherlands

Keywords: Correlation, Differential Phase Shift Keying, Fourier Transforms, Frequency Division Multiplexing, Modulation.

Abstract: Existing communication standards have limited capabilities to adapt to low SNR environments or to exploit low data rate requirements in a power efficient way. Existing techniques like e.g. control coding do not reduce the computational load when reducing data rates. In this paper, we introduce differential Extended Symbol OFDM (differential ES-OFDM) which is based on the transmission of symbols that are extended in time. This way it can operate at low SNR. Using differential BPSK modulation, approximately 2.1 dB SNR improvement per doubling of the symbol length (halving the bitrate) is obtained. The sensitivity to frequency offsets of differential ES-OFDM is basically independent of symbol extension. Extending symbols reduces the computational load on the radio modem within the transmitter which is essential to reduce overall power consumption. The differential ES-OFDM receiver architecture also offers opportunities to reduce power consumption.

1 INTRODUCTION

A general trend in modern society is an increasing emphasis on considerate use of resources, a trend which can also be observed within Wireless Communications. Besides the reduction of direct energy consumption, one of the aims is to reduce the polution of the EM spectrum as much as possible to not disturbe other users and to minimize human exposure to EM radiation. Considerate use of resources is applicable to both infrastructure of wireless communications systems (e.g. basestations) as well as handheld devices. For handhelds, an additional incentive to reduce power consumption is increased operational time. For both mobile phones as well as laptops, backlight and the wireless interface use most of the energy, see (Carroll and Heiser, 2010) and (Mahesri and Vardhan, 2005) respectively. Backlight power consumption is generally counteracted with agressive backlight dimming while techniques to reduce power consumption within the wireless interface are less obvious. According to (Carroll and Heiser, 2010) and (Perrucci et al., 2011), to save power within handheld devices and to reduce EM radiation, one should concentrate on the wireless radio interface of transmitters. This interface can be separated into the Power Amplifier (PA) and the radio modem which runs the transceiver algorithms (physical layer) and Medium Access Control protocols (MAC layer). To reduce power consumption in a wireless radio transmitter interface, the power consumption in the PA and the power consumed by the radio modem should be reduced evenly (Rantala et al., 2009).

In OFDM systems, given a specific modulation scheme (e.g. 16-QAM), minimum Signal-to-Noise-Ratio (SNR) constraints have to be satisfied at the receiver to achieve acceptable Bit Error Rates (BERs). In case data rate requirements are reduced, lowering the modulation scheme leads to lower power consumption and lower radiated power levels. Once arrived at the lowest modulation level (BPSK), other techniques have to be used to reduce power levels.

All options mentioned in section 2 result in more complexity at the transmitter and/or receiver thus leading to lower data rates against higher power consumption. This conflicts with our conclusion that, for effective power reduction, both the power transmitted (consumed in the PA) and the power consumed by the radio modems should be reduced. In this paper we propose an OFDM technique which enables the reduction of radiated power levels leading to lower data rates *and* lower power consump-

tion. It is based on differential encoding of data and the extension of symbols in time and we will refer to it as differential Extended Symbol OFDM (differential ES-OFDM). After describing this technique in section 3, a BER analysis is presented in section 4. Using BPSK modulation, theoretical BER curves for AWGN channels are presented. Estimated and simulation results for both AWGN channels and frequency selective Rayleigh fading channels are presented as well. In section 5, the effects of frequency offsets are studied.

2 RELATED WORK

In (Maeda et al., 2002) and (Gaffney et al., 2005), repetition of symbols in time, allowing less power to be transmitted, is analyzed. By means of Maximum Ratio Combining, multiple replicas of symbols are used to minimize the BER. In (Medina and Kobayashi, 2000), repetition of data in the frequency domain is elaborated. Another option to facilitate lower transmit power is to add error-control coding (Haykin, 2001). Besides that, the efficiency of PA's can be increased by reducing the Peak-to-Average-Power Ratio (PAPR) of the signal to be transmitted as is done in e.g. (Harada et al., 2007).

3 DIFFERENTIAL ES-OFDM

A coherent OFDM receiver has to be synchronized to the transmitter in time, frequency and phase. Especially phase synchronization is costly to obtain. Differential modulation disregards the phase information at the expense of SNR performance. Both frequency- and time differential demodulation detection (FDDD and TDDD respectively) can be used in an OFDM system (Lott, 1999). FDDD and TDDD are compared in (Tan and Beaulieu, 2007a) and it is concluded that FDDD is prefered if the normalized doppler spread dominates the normalized delay spread. When symbols are extended in time which we will introduce later on, the normalized doppler spread increases and the normalized delay spread decreases (Tan and Beaulieu, 2007a). This makes FDDD more suited when using time extended symbols.

In Fig. 1, we present a base-band equivalent model of a differential ES-OFDM system.

At the transmitter, a source produces data vector S^d which consists of $N-1$ complex values (indicated as S_f^d, $f = 1, 2, ..., N-1$) where each value is a constellation point from a chosen modulation scheme.
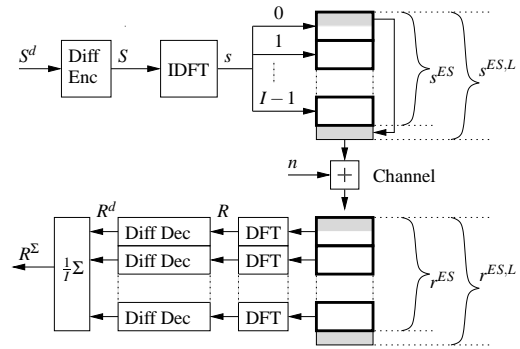

Figure 1: Base-band equivalent model of differential ES-OFDM.

We require that $|S_f^d|$ is constant for all f. S^d is used to modulate carriers S by means of differential encoding

$$S_f = S_{f-1} \cdot S_f^d, \quad f = 1, 2, ..., N-1 \quad (1)$$
$$S_0 = 1 \quad (2)$$

S is transformed into the time domain through the IDFT giving s.

$$s_t = \frac{1}{\sqrt{N}} \sum_{f=0}^{N-1} S_f e^{j\frac{2\pi ft}{N}}, \quad t = 0, 1, ..., N-1 \quad (3)$$

I copies of s are concatenated giving the extended symbol s^{ES}.

$$s_t^{ES} = s_{\text{MOD}(t,N)}, \quad t = 0, 1, ..., IN-1 \quad (4)$$

where $\text{MOD}(,N)$ indicates the modulo N operator. The last L samples of s ($L \leq N$) act as a cyclic prefix completing $s^{ES,L}$. The values of this extended symbol are shifted out serially and transmitted through the channel. We assume an additive white Gaussian noise (AWGN) channel adding n to $s^{ES,L}$ resulting in $r^{ES,L}$.

$$r_t^{ES,L} = s_t^{ES,L} + n_t, \quad t = 0, 1, ..., IN-1 \quad (5)$$

In the receiver, the first step is to remove the cyclic prefix. The resulting extended symbol is r^{ES}. At the receiver, we identify I blocks, where each block contains N samples

$$r_{t,i} = r_{t+iN}^{ES},$$
$$t = 0, 1, ..., N-1 \quad \text{and} \quad i = 0, 1, ..., I-1 \quad (6)$$

Each individual block is converted into the frequency domain. Since the DFT is a linear operation, the signal and noise parts can be separated.

$$R_{f,i} = \text{DFT}(r_{t,i}) = S_f + N_{f,i},$$
$$f = 0, 1, ..., N-1 \quad \text{and} \quad i = 0, 1, ..., I-1 \quad (7)$$

Each individual block is differentially decoded. This operation is defined as

$$R_{f,i}^d = R_{f,i} \cdot R_{f-1,i}^*, \quad f = 1, 2, ..., N-1 \quad (8)$$

where $*$ indicates the complex conjugate. From the I blocks of data, corresponding values are averaged:

$$R_f^\Sigma = \frac{1}{I} \sum_{i=0}^{I-1} R_{f,i}^d \qquad (9)$$

Neglecting the noise contributions, assuming channel gain equals 1 and using (1) to (9), we see that the output of the receiver equals

$$R_f^\Sigma = |S_{f-1}|^2 S_f^d = S_f^d \qquad (10)$$

which is the transmitter input.

To asses the computational complexity of ES-OFDM, we note that, at the transmitter, the rate at which IDFTs are executed is reduced with a factor I. The same holds for the differential encoding. We conclude that the average power consumption at the transmitter is lowered. At the receiver however, the number of DFTs and differential decoding operations is independent of I. Compared to 'normal' OFDM (I=1), the rate of operations at the ES-OFDM receiver is slightly increased because of the summation of I decoded symbols leading to a slightly higher power consumption at the receiver.

4 BIT ERROR RATES FOR DIFFERENTIAL ES-OFDM

SNR performances of differentially modulated carriers in AWGN and fading environments have been studied in e.g. (Miller and Lee, 1998). SNR performance of differential OFDM systems has been studied in (Tan and Beaulieu, 2007a). However, in these analyses, the symbol length is fixed and the results are not applicable in case of extended symbols. Our approach is based on the observation that, although it is common to describe a differential OFDM receiver as an FFT followed by a crosscorrelation, the order of these functions can be exchanged. Restricting ourselves to BPSK modulation, this allows us to use the results presented in (Simon and Divsalar, 1992). In that paper, a continuous time domain analysis of a DPSK demodulator in case of an AWGN channel is presented where a bandpass filtered signal is correlated with a delayed version of the same signal. In Appendix A, we rewrite (9) in such way that, for each carrier f, R_f^Σ is the result of the (cross-)correlation of two modulated carriers. Because of the orthogonality of the carriers, a differential ES-OFDM receiver can be considered as $N-1$ parallel DPSK demodulators.

In the expression presented in (Simon and Divsalar, 1992) relating SNR to BER, two parameters are important. First, the energy per bit over noise
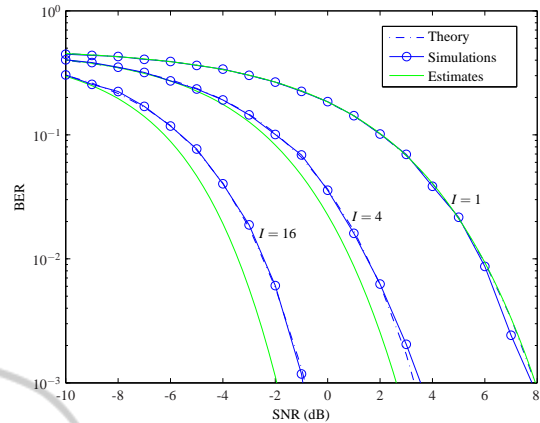

Figure 2: BERs for differential ES-OFDM for an AWGN channel.

spectral density ratio ($\frac{E}{N_0}$) and second the product of the bandwidth of the bandpass filter and the integration time (FT). For differential ES-OFDM using BPSK, the energy per bit over noise spectral density ratio equals SNR$\cdot I$ and the bandwidth-integration time product equals $\Delta f \cdot \frac{NI}{N\Delta f} = I$, where Δf is the inter-carrier spacing. The final result of (Simon and Divsalar, 1992), in case of differential ES-OFDM using BPSK and an AWGN channel, becomes

$$\text{BER} = \frac{1}{2^I} e^{-(I\cdot\text{SNR})} \sum_{i=0}^{I-1} \frac{(I \cdot \text{SNR})^i}{i!} \sum_{j=i}^{I-1} \frac{1}{2^j} C_{j-i}^{j+I-1} \qquad (11)$$

$$C_k^n = \frac{n!}{k!(n-k)!} \qquad (12)$$

This expression can be used to determine the theoretical BER for differential ES-OFDM in case of an AWGN channel. A simulation model has been implemented as well for a system with 64 carriers ($N = 64$), a cyclic prefix length of 8 ($L = 8$), $I = 1, 4$ and 16. The results are presented in Fig. 2 and are labeled with 'Theory' and 'Simulations'. We see that theory and simulation correspond and BER performance increases for increasing I.

To explain the SNR improvement as a function of I, (11) does not give much insight except for $I = 1$ in which case it reduces to the standard relation between SNR and BER for AWGN channels (Haykin, 2001). We therefore derived an estimate of the relation between SNR and BER as a function of I in Appendix B:

$$\text{BER} \approx 0.5 * e^{-\text{SNR}_{\text{EQ}}} \qquad (13)$$

where

$$\text{SNR}_{\text{EQ}} = \frac{I \cdot \text{SNR}^2 + \text{SNR}\sqrt{(I \cdot \text{SNR})^2 + 2I \cdot \text{SNR} + I}}{2 \cdot \text{SNR} + 1} \qquad (14)$$
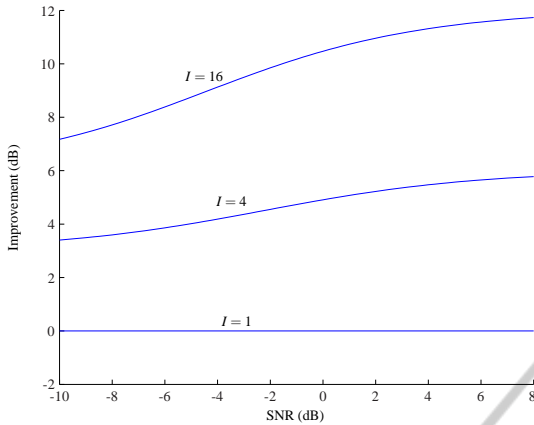
259

Figure 3: SNR improvement for extension factors $I = 1$, 4 and 16.

Figure 4: BERs for differential ES-OFDM for an AWGN (top) and a 7-tap frequency selective Rayleigh fading channel (bottom).

We see that increasing I does not lead to a constant equivalent improvement of SNR_{EQ} but leads to an SNR dependent improvement. The improvement of the equivalent SNR_{EQ}, for $I = 1$, 4 and 16 is presented in Fig. 3.

For the trivial case where $I = 1$, no improvement is obtained. For high SNR, $I = 4$ and $I = 16$, the SNR improvement is close to the maximum improvement of 3 dB per doubling of I. For lower SNR, the improvement degrades because uncorrelated noise (N_1 and N_2, see Appendix B) become more and more dominant which will, for very low SNR lead to an improvement of 1.5 dB per doubling of I (or equivalently 3 dB per quadrupling of I). Based on (13), BER estimates for $I = 1$, 4 and 16 have been added to Fig. 2. The estimates are a bit too optimistic. This is caused by the fact that, especially the signal and noise cross products ($S_1 N_2^*$ and $S_2^* N_1$, see Appendix B), do not resemble an AWGN signal as assumed. Expression (14) has also been used to determine a BER estimate for Rayleigh fading channels based on

$$\text{BER} \approx \frac{1}{2 * (1 + \text{SNR}_{\text{EQ}})} \quad (15)$$

BER estimates, based on (15) are shown in Fig. 4 for $I = 1$, 4 and 16. Simulations have been done for these cases with a 7-tap frequency selective Rayleigh fading channel. These results are also shown in Fig. 4.

Both the simulations and the estimated BER values show that the BER performance improves with increasing I. We also see that the estimate is becoming more and more optimistic for increasing I, similar to the AWGN case.
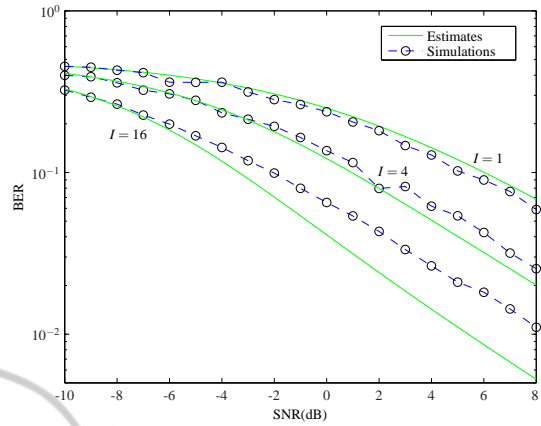
5 FREQUENCY OFFSETS

One of the known disadvantages of OFDM, compared to single carrier systems, is its high sensitivity to frequency offsets. The effects of frequency offsets on frequency-differential modulation have been studied in (Miller and Lee, 1998) and (Tan and Beaulieu, 2007b). In these publications, approximations of the relation between the BER and frequency offsets are given for fixed symbol lengths. In our contribution we concentrate on an approximation of the *relative* effects of symbol extension.

The frequency offset is modeled by multiplying the extended symbol before transmission s^{ES} with a factor $e^{\frac{j2\pi\delta_f t}{N}}$, where δ_f models the frequency offset. We define the signal r_{t,δ_f}^{ES} at the receiver as

$$r_{t,\delta_f}^{ES} = s_t^{ES} \cdot e^{j\frac{2\pi\delta_f t}{N}} + n_t, \quad t = 0, 1, ..., IN - 1 \quad (16)$$

The starting point of the analysis is the correlator output z as defined in (22) of Appendix A. The signal related parts of z are rewritten using (16)

$$z_{\tau,\delta_f} = \frac{1}{IN} \sum_{t=0}^{IN-1} (e^{j\frac{2\pi\delta_f t}{N}} s_t^{ES} \cdot e^{j\frac{2\pi t}{N}})^* \cdot$$
$$e^{j\frac{2\pi\delta_f \text{MOD}(t+\tau,IN)}{N}} s_{\text{MOD}(t+\tau,IN)}^{ES} \quad (17)$$

Ignoring the edge effect where $t + \tau \geq IN$, $e^{j\frac{2\pi\delta_f \text{MOD}(t+\tau,IN)}{N}}$ is approximated by $e^{j\frac{2\pi\delta_f(t+\tau)}{N}}$. Expression 17 then becomes

$$z_{\tau,\delta_f} \approx \frac{1}{IN} e^{j\frac{2\pi\delta_f \tau}{N}} \sum_{t=0}^{IN-1} (s_t^{ES} \cdot e^{j\frac{2\pi t}{N}})^* s_{\text{MOD}(t+\tau,IN)}^{ES} \quad (18)$$

The distorting factor $e^{j\frac{2\pi\delta_f\tau}{N}}$ does not depend on the symbol extension factor I and differential ES-OFDM is therefore, by approximation, insensitive to extended symbol lengths with respect to frequency offsets.

6 CONCLUSIONS

By extending symbols, differential ES-OFDM can achieve acceptable BERs at low SNR. For AWGN and frequency selective Rayleigh fading channels, the SNR requirement at the receiver to achieve acceptable BERs is lowered when extending symbols (and inherently, lowering the data rate). In case of fixed channel conditions, doubling the symbol length reduces the required radiated power level at the transmitter with approximately 2.1 dB. This way power consumption within the PA is reduced. When extending symbols, the computational load per unit time reduces almost proportionally for the transmitter. We thus satisfy the requirement that the power consumed in both the PA and the radio modem of the transmitter should be reduced.

The computational load at the receiver slightly increases when extending symbols if we consider the receiver model presented in Fig. 1. However, as already indicated in our analysis in Section 4, the receiver architecture can also be changed into a crosscorrelation followed by an FFT. In (Kokkeler and Smit, 2011), it is shown that such a receiver architecture can be simplified by reducing the resolution of the Analog-to-Digital Converters giving ample opportunities to lower the power consumption of the receiver. This is still a subject of further research.

REFERENCES

Carroll, A. and Heiser, G. (2010). An analysis of power consumption in a smartphone. In *Proceedings of the 2010 USENIX conference on USENIX annual technical conference*, USENIXATC'10, pages 21–21, Berkeley, CA, USA. USENIX Association.

Gaffney, B., Fagan, A., and Rickard, S. (2005). Upper bound on the probability of error for repetition mb-ofdm in the rayleigh fading channel. *Ultra-Wideband, 2005. ICU 2005. 2005 IEEE International Conference on*, pages 4 pp.–.

Harada, M., Yamamoto, T., Okada, H., Katayama, M., and Ogawa, A. (2007). Reducing peak power for coded ofdm systems by multiple symbol mapping. *Electronics and Communications in Japan (Part III: Fundamental Electronic Science)*, 90(3):67–76.

Haykin, S. (2001). *Communication Systems*. John Wiley & Sons, Inc., fourth edition.

Kokkeler, A. and Smit, G. (2011). A correlating receiver for ofdm at low snr. In *IEEE 73rd Vehicular Technology Conference: VTC2011 - Spring*.

Lott, M. (1999). Comparision of frequency and time domain differential modulation in an ofdm system for wireless atm. *Vehicular Technology Conference, 1999 IEEE 49th*, 2:877–883 vol.2.

Maeda, N., Atarashi, H., Abeta, S., and Sawahashi, M. (2002). Throughput comparison between vsf-ofcdm and ofdm considering effect of sectorization in forward link broadband packet wireless access. *Vehicular Technology Conference, 2002. Proceedings. VTC 2002-Fall. 2002 IEEE 56th*, 1:47–51 vol.1.

Mahesri, A. and Vardhan, V. (2005). Power consumption breakdown on a modern laptop. 3471:165–180.

Medina, L. and Kobayashi, H. (2000). Proposal of ofdm system with data repetition. *Vehicular Technology Conference, 2000. IEEE VTS-Fall VTC 2000. 52nd*, 1:352–357 vol.1.

Miller, L. and Lee, J. (1998). Ber expressions for differentially detected pi;/4 dqpsk modulation. *Communications, IEEE Transactions on*, 46(1):71 –81.

Perrucci, G., Fitzek, H. F., and Widmer, J. (2011). Survey on energy consumption entities on smartphone platform. In *IEEE 73rd Vehicular Technology Conference: VTC2011 - Spring*.

Rantala, E., Karppanen, A., Granlund, S., and Sarolahti, P. (2009). Modeling energy efficiency in wireless internet communication. In *Proceedings of the 1st ACM workshop on Networking, systems, and applications for mobile handhelds*, MobiHeld '09, pages 67–68, New York, NY, USA. ACM.

Simon, M. and Divsalar, D. (1992). On the implementation and performance of single and double differential detection schemes. *Communications, IEEE Transactions on*, 40(2):278–291.

Tan, P. and Beaulieu, N. (2007a). Accurate ber performance comparison of frequency domain and time domain π/4-dqpsk ofdm systems. *Electrical and Computer Engineering, 2007. CCECE 2007. Canadian Conference on*, pages 195 –201.

Tan, P. and Beaulieu, N. (2007b). Precise ber analysis of π/4-dqpsk ofdm with carrier frequency offset over frequency selective fast fading channels. *Wireless Communications, IEEE Transactions on*, 6(10):3770 –3780.

APPENDIX A

The expressions given in section 3 describe a differential ES-OFDM receiver using a so-called FX correlator. In this appendix, we will rearrange the expressions in such way that the receiver describes an XF correlator. Using the shift theorem and (8), (9) can be

rewritten as

$$R_f^\Sigma = \frac{1}{I}\sum_{i=0}^{I-1} R_{f,i} \cdot R_{f-1,i}^* = \frac{1}{I}\sum_{i=0}^{I-1} R_{f-1,i}^* \cdot R_{f,i}$$

$$= \frac{1}{I}\sum_{i=0}^{I-1}\left(\frac{1}{\sqrt{N}}\sum_{t_1=0}^{N-1}\left(r_{t_1,i}e^{j\frac{2\pi t_1}{N}}\right)^* e^{j\frac{2\pi f t_1}{N}}\right) \quad (19)$$

$$\cdot \left(\frac{1}{\sqrt{N}}\sum_{t_2=0}^{N-1} r_{t_2,i}e^{-j\frac{2\pi f t_2}{N}}\right)$$

The summation over t_2 can start at any index within a symbol. We choose to add t_1 to the index.

$$R_f^\Sigma = \frac{1}{IN}\sum_{i=0}^{I-1}\sum_{t_1=0}^{N-1}\left(r_{t_1,i}e^{j\frac{2\pi t_1}{N}}\right)^* e^{j\frac{2\pi f t_1}{N}}$$

$$\cdot \left(\sum_{t_2=0}^{N-1} r_{(t_1+t_2),i}e^{-j\frac{2\pi f(t_1+t_2)}{N}}\right) \quad (20)$$

If we define $t_1 + iN = t$, $t_2 = \tau$ and use (6), (20) becomes

$$R_f^\Sigma = \frac{1}{IN}\sum_{t=0}^{IN-1}\left(r_t^{ES}e^{j\frac{2\pi t}{N}}\right)^* e^{j\frac{2\pi f t}{N}}$$

$$\cdot \left(\sum_{\tau=0}^{N-1} r_{\mathrm{MOD}(t+\tau,IN)}^{ES} e^{-j\frac{2\pi f(t+\tau)}{N}}\right) \quad (21)$$

The exponential parts dependent on t can be removed, and by exchanging the summation order, (21) becomes

$$R_f^\Sigma = \sum_{\tau=0}^{N-1}\left(\frac{1}{IN}\sum_{t=0}^{IN-1}\left(r_t^{ES}e^{j\frac{2\pi t}{N}}\right)^*\right.$$

$$\left. \cdot r_{\mathrm{MOD}(t+\tau,IN)}^{ES}\right) \cdot e^{-j\frac{2\pi f \tau}{N}} \triangleq \sqrt{N}\cdot\mathrm{DFT}(z_\tau) \quad (22)$$

We see that R_f^Σ is proportional to the DFT of a cross-correlation result z_τ. To produce z_τ, the received extended symbol r^{ES} is correlated with a frequency shifted version of the same symbol. The frequency shift corresponds to one carrier spacing.

APPENDIX B

The starting point is the general blockdiagram of a DPSK demodulator presented in Fig. 5. In this figure, S_1 and S_2 represent the differentially encoded signals. N_1 and N_2 are produced by uncorrelated noise sources. We assume that the variances of the signals and noise sources equal σ_S^2 and σ_N^2 respectively. The SNR at each input of the multiplier thus equals $\frac{\sigma_S^2}{\sigma_N^2}$. The two sums $S_1 + N_1$ and $S_2 + N_2$ are multiplied and averaged over IN samples. This average is then fed
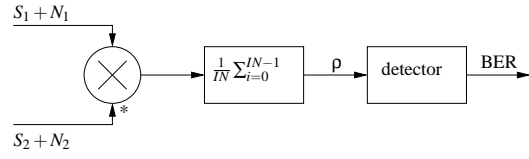

Figure 5: General blockdiagram of a DPSK receiver.

into the detector. Expression 11 describes the relation between the SNR of the input signal and the BER at the output of the detector as a function of I. When keeping the SNR at both inputs of the multiplier constant, increasing I will lead to a higher signal-to-noise ratio ρ at the input of the detector and a lower BER at the output of the detector. To estimate the effect of increasing I, we assume that the SNR improvement at the input of the detector is not caused by increasing I (we assume $I = 1$) but by an increased SNR at both input of the multiplier. The standard relation between SNR and BER as given in (Haykin, 2001) is used to estimate the effect of I.

The signal at the output of the multiplier (see Fig. 5) consists of 4 parts: the signal related part ($S_1 S_2^*$) and three noise related parts ($S_1 N_2^*$, $S_2^* N_1$, and $N_1 N_2^*$). After averaging, we assume that the noise related parts show Gaussian behavior. In case $I = 1$, the signal-to-noise ratio ρ at the input of the detector is approximated by

$$\rho_{I=1} \approx \frac{\sigma_S^4}{2\cdot\sigma_S^2\sigma_N^2 + \sigma_N^4} = \frac{\mathrm{SNR}^2}{2\cdot\mathrm{SNR}+1} \quad (23)$$

Extending the symbol increases ρ with a factor I. To determine the signal-to-noise ratio of a non-extended input signal ($\mathrm{SNR_{EQ}}$) that results in the same ρ as when extending a symbol with I, we formulate the following equation

$$\frac{(\mathrm{SNR_{EQ}})^2}{2\cdot\mathrm{SNR_{EQ}}+1} = \frac{I\cdot\mathrm{SNR}^2}{2\cdot\mathrm{SNR}+1} = \rho_I \quad (24)$$

Rewriting this equation leads to the following solution:

$$\mathrm{SNR_{EQ}} = \frac{I\cdot\mathrm{SNR}^2 + \mathrm{SNR}\sqrt{(I\cdot\mathrm{SNR})^2 + 2I\cdot\mathrm{SNR}+I}}{2\cdot\mathrm{SNR}+1} \quad (25)$$

The estimate of the equivalent SNR can be used within the well known BER expressions (see (Haykin, 2001)) for both AWGN and Rayleigh fading channels. For AWGN channels, this leads to the following expression

$$\mathrm{BER} \approx 0.5 * e^{-\mathrm{SNR_{EQ}}} \quad (26)$$